

# MAXIMIZING BRIGHTNESS IN PHOTOINJECTORS \*

C.Limborg-Deprey, SLAC, 2275 Sand Hill Road, MS18, Menlo Park, US

## Abstract

If the laser pulse driving photoinjectors could be arbitrarily shaped, the emittance growth induced by space charge effects could be totally compensated for. In particular, for RF guns the photo-electron distribution leaving the cathode should have a 3D-ellipsoidal shape. The emittance at the end of the injector could be as small as the cathode emittance. We explore how the emittance and the brightness can be optimized for photoinjector based on RF gun depending on the peak current requirements. Techniques available to produce those ideal laser pulse shapes are also discussed.

## INTRODUCTION

The high brightness quality of beam produced in RF photoinjectors comes from the possibility of achieving very good emittance compensation [1].

After emittance compensation, the total emittance has four contributions, the cathode emittance, the non-linear space charge emittance, the RF emittance and the chromatic emittance as shown in Eq. (1).

$$\epsilon_{tot} = \sqrt{\epsilon_{cathode}^2 + \epsilon_{RF}^2 + \epsilon_{chrom.}^2 + \epsilon_{non-lin. space\ charge}^2} \quad (1)$$

For the two types of photoinjectors discussed in this paper [2,3], which plan to use flat top laser distributions, the cathode emittance and the non-linear space charge emittance each share half of the emittance budget, while the other contributions are nearly negligible. A small RF emittance is the consequence of the short pulse lengths (about 10-15 degrees for the S-Band and L-Band systems discussed in this paper) required to meet high peak currents (~50-100 A) at the end of the injector. The non-linear space charge emittance can be totally suppressed by using 3D-ellipsoidal laser pulses. The total emittance is then only the cathode emittance. Beam dynamics in photoinjector driven by 3D-ellipsoidal laser pulses are reviewed. Optimization of photoinjectors based on S-Band guns is discussed for charges varying from 0.2 nC to as high as 10 nC. The very promising results obtained from simulations suggest that the effort required to produce 3D-ellipsoidal laser pulses is worthwhile.

## EMITTANCE

### Cathode Emittance

The “thermal emittance” can be computed based on the laser energy and the surface barrier potential, and the electron affinity for the semi-conductor cathode material [4]. For copper cathode, most common material for S-Band guns, the “thermal emittance” per unit spot radius is 0.3  $\mu\text{m}$  per mm. For Cs<sub>2</sub>Te, most common material for L-Band guns, the “thermal emittance” is estimated to be 0.43  $\mu\text{m}$ . Several electron beam based measurements have

shown that the “cathode emittance” is larger than the “thermal emittance”. For both copper and Cs<sub>2</sub>Te the measured value is close to 0.6 mm per mm radius [5,6]. Many reasons could explain the difference between the “cathode emittance”, which is a measured quantity, and the “thermal emittance” which is a theoretical value, such as surface roughness, scattering of the electrons, oxidation of the surface, two-photon absorption ...

The “cathode emittance” is proportional to the radius,  $r$ , of the laser spot. A radius as small as possible is desirable. However, the limit on the radius is imposed by the image space charge limit at the cathode or by non-linear space charge forces. Those latter usually force the radius for cylindrical pulses. As they are absent in the case of 3D-ellipsoidal pulse, the image charge limits the minimum radius, which in turn allows lower values than what is usually used for cylindrical pulses. The space charge limit is described by the two equations of formula (2). They express the fact that the accelerating field on the cathode,  $E_{RF}$ , needs to overcome the image charge field  $E_s$  given by Gauss’s law.

$$|E_{rf}| > |E_s| \text{ with } E_s = \frac{c}{\epsilon_o} = \frac{Q}{\pi r^2 \epsilon_o} \quad (2)$$

$Q$  is the bunch charge,  $\epsilon_o$  is the vacuum permittivity.

Typically for a 1 nC charge and a 1 mm radius spot size, the cathode field needs to exceed 36 MV/m. For a 30 degree operating phase, the field should be of at least of 72 MV/m. The operating phases need to be in the 20-40 degrees range to have a small energy spread to achieve good emittance compensation.

### RF Emittance

The RF emittance has been described analytically in [7]. Its scaling is reproduced in Eq. (3), which shows that it is proportional to the product of the beam volume by the rms bunch length,  $\sigma_z$ . This emittance is 0.05  $\mu\text{m}$  for the LCLS nominal parameters.  $f_{rf}$  is the gun RF frequency.

$$\epsilon_{RF} \sim \frac{E_{peak}}{f_{rf}} \sigma_r^2 \sigma_z^2 \quad (3)$$

### Chromatic Emittance

The chromatic emittance is a consequence of the energy dependence of the solenoid focusing. Eq. (4) shows that it is proportional to the energy spread,  $(\Delta p/p)$ , the square of the rms beam size  $\sigma_r$ , and the inverse of the solenoid focal length,  $f$ .

$$\epsilon_{chrom.} \propto \frac{\Delta p}{p} \frac{\sigma_r^2}{f} \quad (4)$$

Since the space charge induced emittance growth can totally be suppressed with ellipsoidal pulses, the combination of RF and chromatic emittances can be evaluated numerically by setting to zero the “cathode emittance”. For our LCLS case, it was determined to be of  $0.15 \mu\text{m}$  for the 1 nC case with 1.2 mm radius and 10 ps of cylindrical beam. Obviously, this method slightly underestimates the value when space charge is present.

### Non-linear Space Charge Emittance

The non-linear space charge emittance scales like the charge density and depends on a form factor,  $F$ . For a 3D-ellipsoidal uniform pulse, the form factor  $F$  is equal to zero. For all other pulses, the form factor  $F$  depends on the shape and uniformity of the laser distribution.

For the cylindrical shape laser pulse, the optimum radius results from a compromise between tolerable space charge force, which is synonymous of non-linear space charge, and “cathode emittance”,  $\mathcal{E}_{cathode}$ , normalized to laser spot size. This compromise is summarized in Eq. (5).

$$\mathcal{E}_{tot} = \sqrt{(\mathcal{E}_{cathode} \sigma_r)^2 + (F \frac{Q}{\sigma_r^2 \sigma_z})^2} \quad (5)$$

### LCLS nominal case

For the LCLS photoinjector, the optimum tuning corresponds to an equal combination of “cathode emittance” (for  $0.7 \mu\text{m}$ ) and non-linear space charge emittance (for  $0.7 \mu\text{m}$ ). The total emittance is  $1 \mu\text{m}$ . A smaller emittance of  $0.85 \mu\text{m}$  can be obtained if the “cathode emittance” is reduced to  $0.5 \mu\text{m}$  by using a radius of  $0.85 \text{ mm}$  instead of  $1.2 \text{ mm}$ . But the laser pulse length has to be stretched to a 20-ps pulse duration [8]; and the peak current is then 60 A instead of the required 100 A peak current. The  $0.85 \mu\text{m}$  is the ultimate minimum for the LCLS injector run with 1 nC because a further reduction of the radius requires longer bunches and which increases the RF emittance to a significant level, following the scaling law already presented with Eq. (3).

## 3D-ELLIPSOIDAL PULSES

An X-Ray FEL injector needs to provide a beam with about constant slice emittance along the beam and similar peak current for the SASE mechanism to be optimum for as many slices as possible along the bunch. Accordingly, flat top distributions have been the preferred option until now. However, even better beam performances, both in emittance and brightness, could be obtained if a 3D-ellipsoidal laser pulse could be used as the photoinjector laser driver pulse.

### Beam dynamics

Figs. 2, 3 and 4 illustrate the benefits of this modification. In Figs. 2 and 3, we compare the evolution of the transverse phase space, the longitudinal phase space and the focusing parameter  $r'/r$  for the cylindrical pulse, as in Fig. 1, and for the 3D-ellipsoidal pulse in Fig 2. The first line shows the beam distribution at the exit of the

gun, i.e., at the location where the solenoid starts refocusing the beam, and the second line shows the distribution when the beam is entering the linac, i.e., when the emittance compensation is nearly completed. The seven longitudinal slices have been color coded. The suppression of the non-linear space charge force for the 3D-ellipsoidal distribution is visible in the  $r'/r$ -graph. The  $r'/r$  becomes very non-linear at the head and tail of the cylindrical beam since the longitudinal space charge force distorts the square shape longitudinal shape into a parabolic one, varying the charge density with respect to that of the longitudinal core of the bunch. For the 3D-ellipsoidal bunch, the charge density remains constant over the whole volume of the bunch as the beam is transported. The impressive reduction of slice emittance and increase in peak brightness for the 3D-ellipsoidal shape bunch compared to the cylindrical one are given in Figs. 3 (a) and (c). Fig. 3 (b) shows that the peak current profile of the 3D-ellipsoidal reaches nearly the same level as that of the cylindrical shape. Finally, in Fig. 3 (d), the very linear longitudinal phase space of the 3D-ellipsoidal beam is compared to that of the cylindrical beam; the 2<sup>nd</sup> order term coming from the RF curvature has been removed. The linearity of the longitudinal phase space will allow reducing the strength of the high harmonic linearization which precedes the bunch compressors.

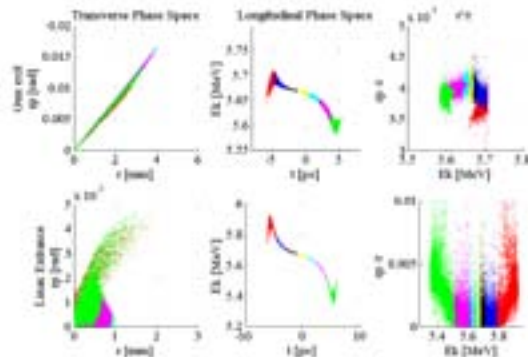


Figure 1: Emittance compensation for a cylindrical shape beam

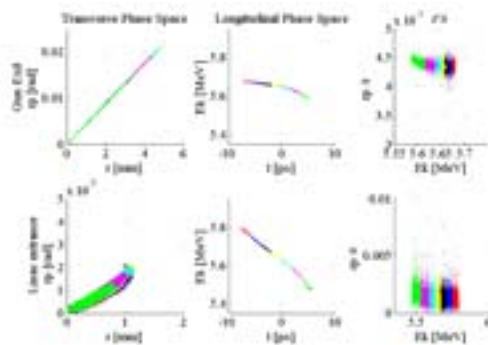


Figure 2: Emittance compensation for a 3D ellipsoidal laser distribution

## OPTIMIZATION

The optimization of a beamline requires optimizing the laser beam volume and the beamline parameters to minimize the final projected emittance and provide a beam size slightly convergent. The search for small emittance is done in the context of a peak current constrained by the overall accelerator.

### S-Band

A comparison of the best optimization of the LCLS photoinjector beamline for the 1 nC charge for both the cylindrical and 3D-ellipsoidal cases are shown in Fig 3. This optimization was obtained for a 120 MV/m gun peak field and a cathode emittance of 0.6  $\mu\text{m}$  per mm.

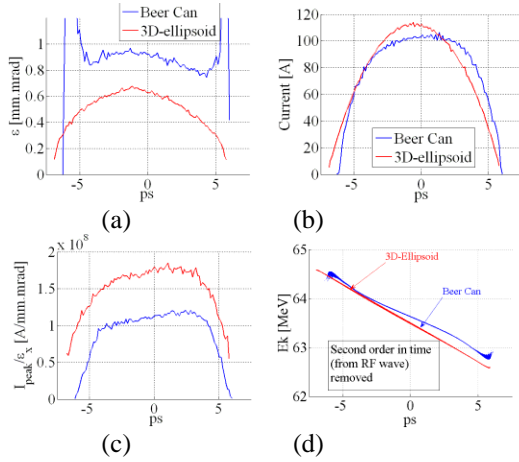


Figure 3: Comparison of beam parameters for 3D-ellipsoidal distribution and cylindrical beam.

### L-Band

The optimization presented in Fig. 4 compares the cylindrical shape and the 3D-ellipsoidal case for the TTF2 layout. The RF gun peak field is 40 MV/m and the cathode emittance is 0.43  $\mu\text{m}$  per mm.

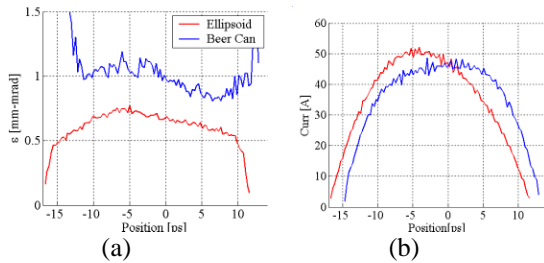


Figure 4: Comparison slice emittance (a) and peak current (b) for 3D-ellipsoidal distribution and cylindrical beam.

The improvement of the stability of the emittance with variation of the parameters has been described in [9] and is not reproduced here by lack of time.

### Optimum brightness

The brightness scales like the ratio of the peak current over the square of the emittance. Determining numerically the optimum brightness is difficult as it requires finding the combination of small emittance and high peak current.

The study, presented here first, focused on minimizing the emittances using ideal ellipsoidal laser shapes. For a few of the points of Figs. 6-7, an attempt to increase the peak current resulted in larger emittances, and above all larger brightnesses. The author plans to devote more time to complete the study, but does not expect fundamental differences to what is presented here.

The minimization of emittance was performed for the S-Band gun version to be run at the LCLS. As recent modifications implemented on the LCLS gun [10] should allow 140 MV/m peak field, this value was used in the simulations presented here. Parameters such as the maximum radius, the solenoid strength, the injection phase, the linac gradient were varied. The linac gradient was chosen to meet as well as possible the invariant envelope laminar waist at the entrance of the booster [11].

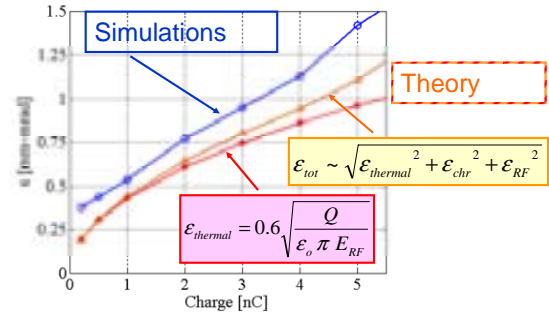


Figure 5: Optimization S-Band gun based photoinjector beamline for charges varying from 0.2 nC to 10 nC. A cathode emittance of 0.6  $\mu\text{m}$  per mm radius spot size has been assumed

## 3D-ELLIPSOIDAL LASER PULSE PRODUCTION

Producing a laser pulse with a radius from zero to the maximum radius and back to zero in less than 10ps, with constant fluence is very challenging. The difficulties of producing uniform 3D-ellipsoidal laser pulses have been described in [9]. We briefly report here on two of the possible solutions and illustrate the expected results with electron beam simulations.

### Pulse stacker

The pulse temporal stacking approach requires the summation or stacking of multiple beamlets, each of which has a specified time delay, transverse radius and pulse energy. Assume that each beamlet is temporally Gaussian but transversally uniform (flattop). Fluence would then be held constant in time only in a discrete way (beamlet peak-to-beamlet peak). The summation in the overlap region partially smoothes the discrete fluence levels. Each beamlet must have its own transverse profile shaper with imaged transport downstream of the shaper. Each beamlet must also have independent optical delay and independent pulse energy control. Fluence preservation over all beamlets requires that the energy of a given beamlet scales linearly with its transverse area. The uniform transverse profile guarantees constant

fluence within any beamlet Interference effects will introduce additional intensity and power variations (ripples) which can be minimized by alternating beamlet polarization between ‘S’ and ‘P’ cases. Complexity, size and cost can escalate rapidly with the number of beamlets used (for example, 10 or more). The efficiency of such a system was estimated to be at the  $10^{-2}$  level for UV wavelengths.

In Fig. 6, we compare simulations results obtained for 8 and 12 beamlets. Twelve trials were computed for each case using random phases, between the beamlets.

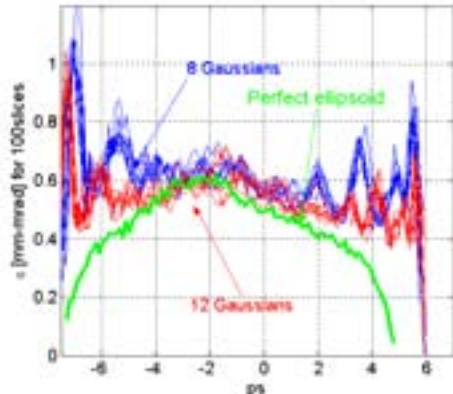


Figure 6: Slice emittance from simulations for a pulse stacker with 8 Gaussians (blue) and 12 Gaussians (red) compared with an ideal 3D-ellipsoidal shape

### Spectral masking

An energy-chirped laser beam reflecting on a grating will project its energy-time dimension into a spatial dimension. The efficacy of spectral masking to control the transverse beam shape and diameter can be considered in terms the uniqueness of the time-space (one dimensional) correlation downstream of a diffraction grating in the plane of dispersion. Uniqueness limits are attributed to the nonzero beamsizes projected on the grating and can be evaluated with a uniqueness function,  $U$ . Discussion of the uniqueness function has been given in [8] and proves that such an optical layout allows to generate a elliptical cylinder. The intersection of 4 elliptical cylinders rotated by 45 degrees gives a good approximation of an ellipsoid, with an octagonal cross-section instead of a disk. If the number of such elliptical cylinders is increased to 6, with 30 degrees between them, the approximation is perfect. Results of the beam dynamics for these two configurations are given in Fig. 7.

The efficiency of a 2 stage (8 gratings) configuration is unfortunately estimated to be as low  $10^{-10}$ .

## CONCLUSIONS

The great improvement of emittance and brightness performances when using 3D-ellipsoidal laser pulses instead of cylindrical shapes has been demonstrated. For 3D-ellipsoidal laser pulses, we demonstrated that the

maximum peak brightness follows is in fact obtained in for 0.5 nC for the S-Band gun.

The great benefits of such pulses make them worthwhile investigating thoroughly the possibility of producing them. Another possibility to produce ellipsoidal emitted electron bunches is described in [12].

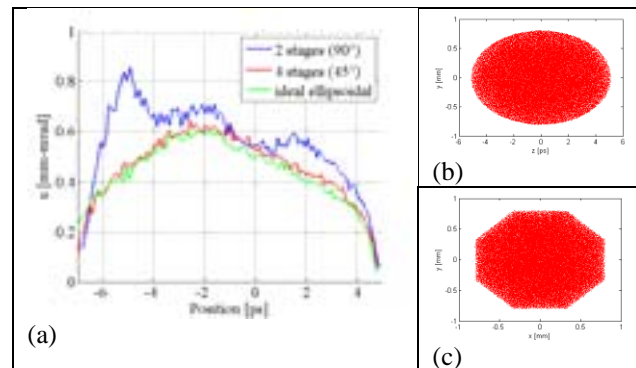


Figure 7: (a) Slice emittance from simulations from pulse built with spectral masking. The cross section of the 4 stage configuration are given in (b) for the z-y plane and (c) for the x-y plane.

## REFERENCES

- [1] B.Carlsen, “New Photoelectric Injector Design for the Los Alamos National Laboratory XUV FEL Accelerator”, NIM A285 (1989) 313-319
- [2] LCLS Photoinjector, [http://www-ssrl.slac.stanford.edu/lcls/cdr/lcls\\_cdr-ch06.pdf](http://www-ssrl.slac.stanford.edu/lcls/cdr/lcls_cdr-ch06.pdf)
- [3] TESLA Photoinjector, [http://tesla.desy.de/new\\_pages/TDR\\_CD/PartII/accel.html](http://tesla.desy.de/new_pages/TDR_CD/PartII/accel.html)
- [4] K.Floettmann, “Note on the Thermal Emittance of Electrons Emitted by Cesium Telluride Photo Cathodes”, Feb 1997, TESLA-FEL, 97-01
- [5] W.Graves et al., “Measurement of Thermal Emittance for a copper PhotoCathode”, PAC01 Proceedings
- [6] V.Mitchell, “Thermal Emittance Measurements”, ICFA X-Ray FELs Commissioning workshop, Zeuthen April 2005
- [7] K.J.Kim, “RF and space charge effects in laser driven RF electron guns”. NIM in Physics Research A275 (1989) 201-218
- [8] C.Limborg-Deprey et al., “Modifications of the LCLS PhotoInjector Beamline” EPAC 04 Proceedings, Lucerne, July 2004
- [9] C.Limborg-Deprey, “Optimum Electron Distributions For Space Charge Dominated Beams”, ERL05 Proceedings, Jlab, to be published in NIM
- [10] L.Xiao, “Dual Feed RF Gun Design for the LCLS”, PAC 05, Knoxville, USA
- [11] M.Ferrario, “Homodyn study for the LCLS RF Photoinjector”, “Physics of high Brightness beams”, World Scientific (2000), P534
- [12] O.J.Luiten “these proceedings”